INDERSCIENCE PUBLISHERS
Linking academia, business and industry through research

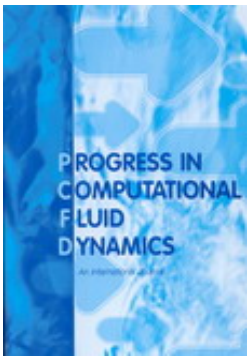

Progress in Computational Fluid Dynamics, An International Journal

ISSN online: 1741-5233 - ISSN print: 1468-4349
https://www.inderscience.com/pcfd

Aerodynamic performance of dragonfly-inspired wings in gliding flight for varying angle of attack and Reynolds number: a numerical study

Prathmesh Verekar, Satish Shenoy Baloor, Hamid Yusoff, Irfan Anjum B. Magami, Sarfaraz Kamangar, Mohammad Zuber

DOI: 10.1504/PCFD.2024.10066254

Article History:

Received:	26 August 2023
Last revised:	17 May 2024
Accepted:	17 May 2024
Published online:	06 January 2025

Aerodynamic performance of dragonfly-inspired wings in gliding flight for varying angle of attack and Reynolds number: a numerical study

Prathmesh Verekar and Satish Shenoy Baloor

Department of Aeronautical and Automobile Engineering,
Manipal Institute of Technology,
Manipal Academy of Higher Education,
Manipal, Karnataka, 576104, India
Email: prathmesh.verekar1@learner.manipal.edu
Email: satish.shenoy@manipal.edu

Hamid Yusoff

Mechanical Engineering Studies,
College of Engineering Universiti Teknologi MARA,
Penang Branch, Permatang Pauh Campus,
13500 Pulau Pinang, Malaysia
Email: hamidyusoff@uitm.edu.my

Irfan Anjum B. Magami and Sarfaraz Kamangar

Mechanical Engineering Department,
College of Engineering,
King Khalid University,
Abha 61421, Saudi Arabia
Email: magami.irfan@gmail.com
Email: sarfaraz.kamangar@gmail.com

Mohammad Zuber*

Department of Aeronautical and Automobile Engineering,
Manipal Institute of Technology,
Manipal Academy of Higher Education,
Manipal, Karnataka, 576104, India
Email: mohammad.zuber@manipal.edu
*Corresponding author

Abstract: This paper numerically investigates the aerodynamic performance of dragonfly-inspired wings for gliding flight. Dragonfly hind wing morphology (planform and thickness) is considered to create a three-dimensional model. The morphology was obtained from the *Aethriamanta brevipennis* (Scarlet Marsh Hawk) species of Odonata using a digital micrometer instrument and scanning electron microscope. Gliding flight is known for energy-saving applications. The present study was conducted to assess the effects of the angle of attack (α) (0° to 40°) on the glide performance. The Reynolds numbers of 550, 1,400, and 10,000 were used. The flow separation was witnessed beyond 10° of the angle of attack, and the peak value of glide ratio was near 10° angle of attack. This study shows that dragonfly will sustain flight at Reynolds number of 550 and 1,400 by orienting its wing for an angle of attack of 10°. This study has potential to aid in developing an appropriate wing orientation for insect-scale aerial vehicle applications.

Keywords: dragonfly; gliding; CFD; wing morphology.

Reference to this paper should be made as follows: Verekar, P., Baloor, S.S., Yusoff, H., Magami, I.A.B., Kamangar, S. and Zuber, M. (2025) 'Aerodynamic performance of dragonfly-inspired wings in gliding flight for varying angle of attack and Reynolds number: a numerical study', *Progress in Computational Fluid Dynamics*, Vol. 25, No. 1, pp.54–61.

Biographical notes: Prathmesh Verekar is a research scholar in the Department of Aeronautical and Automobile Engineering at Manipal Institute of Technology, Manipal, India. His research areas include CFD and fluid mechanics.

Satish Shenoy Baloor is a Professor in the Department of Aeronautical and Automobile Engineering at Manipal Institute of Technology, Manipal, India. His research areas include tribology, FSI for bearings and seals, medical devices, composite materials and biomechanics.

Hamid Yusoff is an Associate Professor in the Mechanical Engineering Studies, College of Engineering Universiti Teknologi MARA, Malaysia. His research areas include micro air vehicles, aerodynamics and experimental fluid.

Irfan Anjum B. Magami is a Professor in the Mechanical Engineering Department, King Khalid University His research areas include heat transfer, CFD, porous media, renewable energy and biomechanics.

Sarfaraz Kamangar is an Assistant Professor in the Mechanical Engineering Department, King Khalid University His research areas include biomechanical, heat transfer, and fluid dynamics.

Mohammad Zuber is a Professor in the Department of Aeronautical and Automobile Engineering at Manipal Institute of Technology, Manipal, India. His research areas include CFD, nasal flow studies and heat transfer.

1 Introduction

Early success in achieving heavier-than-air flight started with non-powered gliding (Gibbs-Smith, 1974; Jakab, 2012). It is commonly seen in biological flappers and unmanned aerial vehicle flights as it is energy efficient (Sachs, 2017, 2022; Mizrahy-Rewald et al., 2022). Birds are remarkable gliders, and they have the ability to use the air currents for sustained flight (Sachs, 2022). Gliding involves reducing the active flapping of wings and using air currents to achieve forward motion with minimal energy expenditure. Gliding flight is characterised by lift to drag ratio, the flow over the airfoil, and flow separation at a high angle of attack (α). Flow separation at a higher angle of attack leads to stall. There are various studies (Livya et al., 2015; Sett et al., 2023; Singh et al., 2023a) to delay stall. Bioinspired wings are known for high lift and low Reynolds number flight (Boughou et al., 2023). Though insect gliding is not very common, dragonflies are known to be good gliders.

Dragonflies survive by hunting during flight, for which they have developed complex aerodynamic mechanisms and biological morphology. The wings of dragonflies can be individually controlled, which is possible due to the direct muscles attached to the wing joints (Simmons, 1977). The control of individual wings allows manoeuvring in all directions, inspiring researchers to mimic its flight (Gaissert et al., 2013; Bin Abas et al., 2016; Singh et al., 2022, 2023b). Individual control also enables them to twist their wings and maintain different orientations for gliding. Gliding flight is commonly seen in birds, then in insects. In dragonflies, gliding is used for thermoregulation, that is, convective cooling, by moving quickly through the air (May, 1978, 1991; Heinrich, 1993). The flow is considered steady for gliding, and steady-state aerodynamic forces are easy to predict and measure (Wakeling and Ellington, 1997).

Computational fluid dynamics is a tool used to provide aerodynamic information around the complex flow involved in different everyday activities. CFD is an effective alternative to physical testing in terms of time and monetary aspects of a study. Applications include the design of spoilers, wings, and lift enhancement surface modifications. CFD is also used to understand complex human fluid flows, the blood flow through arteries (Peskin, 1977; Khader et al., 2018; He et al., 2023), and nasal airflow (Valerian Corda et al., 2023a, 2023b), for example.

Kesel (2000) carried out experiments on dragonfly wings to investigate variations in morphology patterns along the spanwise direction of the wing at three sections. These three sections were separately studied, hence, not capturing the 3D effects of wing morphology variations seen in actual dragonfly wings. In this study, the aerodynamic performance for gliding flight for the dragonfly-inspired wing is numerically investigated for different angles of attack and Reynolds number. The gliding performance is characterised by glide ratio and flow visualisation. For this study, the hind wing of the dragonfly is considered due to its larger posterior area (Wakeling and Ellington, 1997; Rival et al., 2011; Chen and Skote, 2016). According to Chen and Skote (2016), the difference between the corrugated and non-corrugated wings for the low Reynolds number flow was minimal. Hence, the present study has not considered the corrugation. The dragonfly glides under a Reynolds number of 2,400 (Wakeling and Ellington, 1997), thus this study considers 1,400 and 550. Reynolds number of 10,000 is considered for comparison with experimental literature (Kesel, 2000) and computational studies (Chen and Skote, 2016). The paper is structured to address the species-specific model and the methodology to capture the dragonfly wing morphology in Section 2. The numerical methodology adopted in Section 3.

2 Wing morphology

Dragonflies have fascinating wing morphology; in this study, only the planform and thickness variations in the different directions are considered.

Figure 1 SEM image showing the section of the wing, (a) section of dragonfly wing (b) zoomed image showing thickness of the veins (see online version for colours)

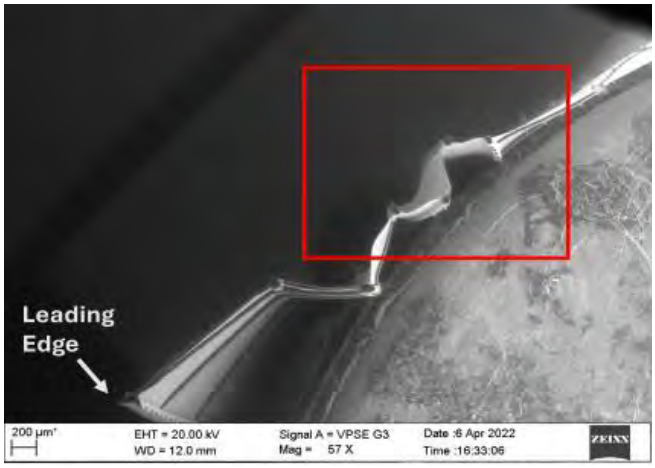

(a)

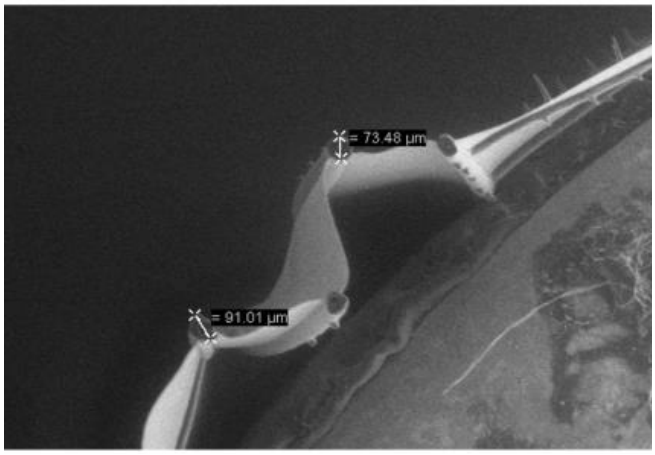

(b)

Different methods are followed in literature (Okamoto et al., 1996; Kesel, 2000; Jongerius and Lentink, 2010) to obtain wing morphology using micro-CT, SEM, and more. This study uses a digital micrometre, a digital camera, and scanning electron microscope (SEM) imaging to capture the wing morphology. This dragonfly specimen [*Aethriamanta brevipennis* (Scarlet Marsh Hawk)] is collected from the garden. The large container is used to collect the insect cadaver, and the smaller containers preserve individual wing samples. The jars are cleaned with an alcohol solution before use to avoid any contamination. Different preservation methods (4 Ways to Preserve Insects – wikiHow, n.d.) include preserving insects in rubbing alcohol, hand sanitizer and pinning insects. The method followed in this study for preservation is a 1:1 solution of water and alcohol.

The wings are photographed using a Canon DSLR on plain white paper and graph paper to capture the wing length and planform. The wing was divided along the spanwise and longitudinal axis to obtain the wing geometry. The wing thickness is measured using a digital micrometer. It is noted that the thickness reduces from the wing root to the wing tip and from the leading edge to the trailing edge, as seen in aircraft wings. This thickness data is further studied using a SEM. The preserved specimen is `then air-dried at room temperature for 24 hours to avoid any distortion of SEM images (Jongerius and Lentink, 2010). The wing sample is cut at a certain wing length using a scalpel blade. Once the wing is cut into sections, these sections are studied under the SEM. The thickness near the leading edge is higher than that near the trailing edge, as seen in Figure 1(a). The thickness of the vein can be seen reducing from 91.01 microns to 73 microns as we move from leading towards the trailing edge in Figure 1(b).

3 Computational methodology

In this section, the domain mesh and simulation setup is explained.

3.1 Geometry and computational domain

Based on the SEM and micrometer data, the three-dimensional model is prepared using Dassault Systemes 3DExperience 2019. The model is a plain profiled hind wing model considering the species characteristic morphology, the planform, and thickness variation along the chord and span of the wing. The model (model 1: profiled HW model) used for this study is shown in Figure 2. Also, it is important to note that the mean chord length (cm) of the wing is 10 mm.

Figure 2 Three-dimensional model

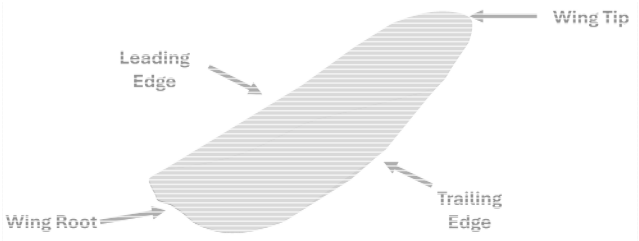

The computational domain consists of two parts: the fine-discretised inner domain and the coarse-discretised outer domain. The outer domain is a cuboid with the upstream dimension at five times the mean chord length and the downstream at 15 times the mean chord length. In the vertical direction, the domain extends to five times the mean chord length in both (positive and negative) directions. The extension in the third direction is eight times the mean chord length from the middle of the wingspan in both directions.

Figure 3 shows the computational domain used. The fine inner domain has a semi-circular region upstream and downstream (at the end). The radius of the semi-circular

region is three times the mean chord length. The upstream consists of only the semi-circular region. Whereas, to capture the wake, the downstream dimension is eight times the mean chord length and ends with a semi-circular region. The extension in the third direction is six times the mean chord length from the middle of the wingspan in both directions.

Figure 3 Computational domain (see online version for colours)

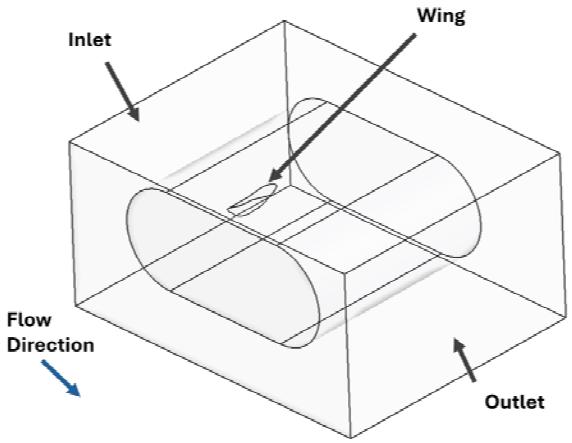

3.2 Mesh

For the meshing, commercial software ANSYS 2022 R1, Fluent with fluent mesh, is used. Polyhedral elements are used. The fine inner domain is meshed using a body of influence with an element size of 2 mm, and the size is chosen based on the mesh convergence study (listed in Table 1). The domain computational grid is shown in Figure 4. Inflation layers were added to capture the boundary layer effects, with the first layer thickness of 0.01 mm considered to have the y plus value of less than 1. Figures 5(a) and 5(b) shows the zoomed mesh near the wing. The maximum aspect ratio is maintained at less than 100. Also, it is important to note that the mean chord length of the wing is 10 mm.

Figure 4 Computational grid

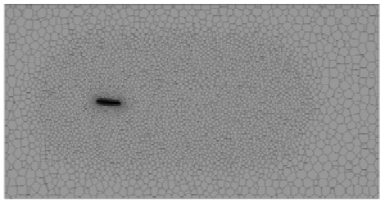

Table 1 Mesh convergence study

Grid	*Volumes*	C_L	C_D	C_L/C_D
3 mm BOI	675,668	0.3072	0.1031	2.9796
2 mm BOI	821,346	0.3069	0.1029	2.9825
1.5 mm BOI	1,077,444	0.3067	0.1026	2.9876
1 mm BOI	2,091,527	0.3057	0.1024	2.9861

Figure 5 Computational grid near wing, (a) computational grid near wing (b) zoomed image showing grid refinement near wing (see online version for colours)

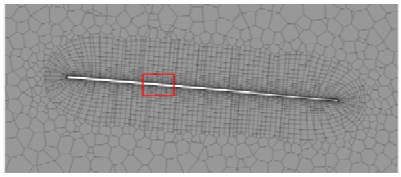

(a)

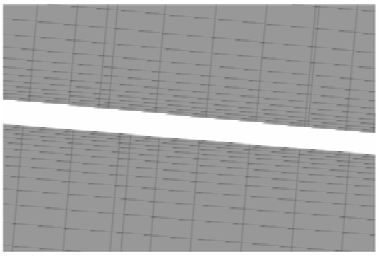

(b)

3.3 Computational setup

For the simulation, second-order discretisation is used. The k-omega SST turbulence model is used for capabilities for low Reynolds number and flow separation applications. The flow conditions and boundary conditions are listed in Table 2.

Table 2 Simulation setting

Specifications	*Parameters used*
Solver used	Pressure based
Model used	Viscous model – K-Omega (SST)
Boundary conditions	Velocity inlet, pressure outlet, no slip for wing wall, and free slip for enclosure domain.
Method used	SIMPLE
Residual monitors (convergence criteria)	Up to 10^{-6}
Initialisation type	Hybrid initialisation
Density	1.225 kg/m^3
Viscosity	$1.789*10^{-5}$ kg/ms
Operating pressure	101,325 Pa
Gauge pressure	0 Pa
Spatial discretisation	Second order upwind

4 Results and discussion

In this study, the gliding performance of the hind wing of the dragonfly was numerically analysed for three Reynolds numbers (550, 1,400, and 10,000), and corresponding gliding speeds are mentioned in Table 3.

We have demonstrated the Wall Yplus values for Reynolds number of 1,400, as seen in Figure 6, which is sufficiently less than 1.

Table 3 Reynolds number with corresponding gliding speed

Reynolds number	*Gliding speed (m/s)*
550	0.8
1,400	2
10,000	15

Figure 6 Wall Yplus for Reynolds number of 1,400 (see online version for colours)

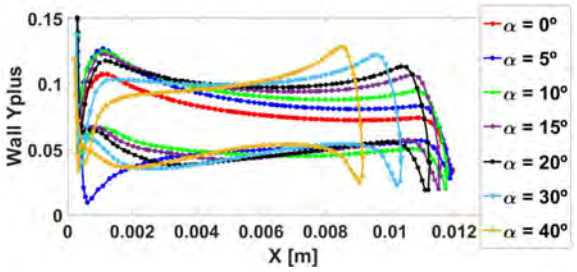

Figure 7 Glide ratio for Reynolds number of 1,400 (see online version for colours)

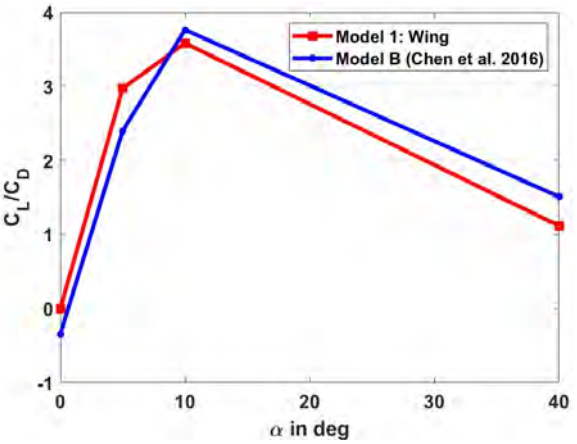

Figure 8 Glide ratio for Reynolds number of 10,000 (see online version for colours)

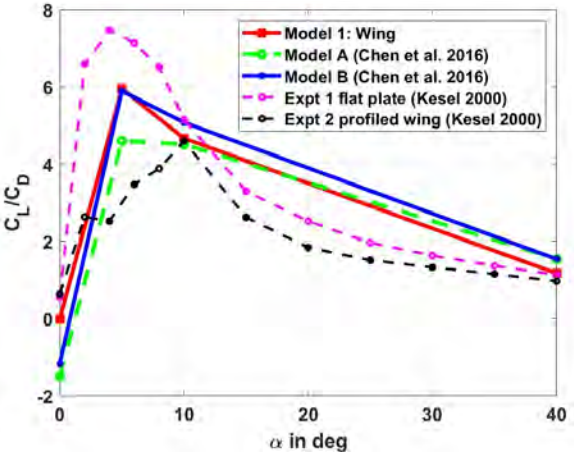

Figure 7 showcases the comparison of the present study with that of Chen and Skote (2016) (model B) for the Reynolds number of 1,400. It can be seen that the finding of the simulation study closely matches with the literature. The minor differences can be attributed to the species differences. In the present study, we introduced '*Aethriamanta brevipennis*' whereas the study by Chen and Skote (2016) used 'Anax Parthenope Julius'.

Figure 9 Glide ratio for Reynolds numbers 550, 1,400 and 10,000 (see online version for colours)

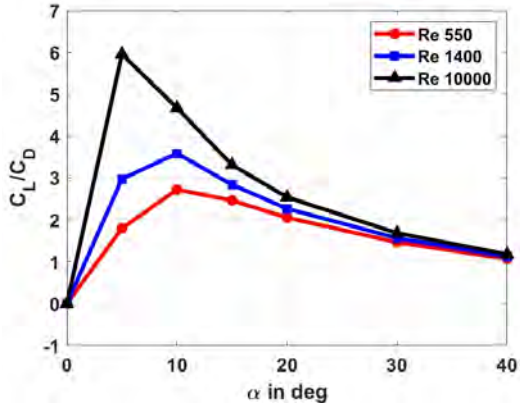

Figure 10 Pressure distribution over the wing for Re 1,400 (see online version for colours)

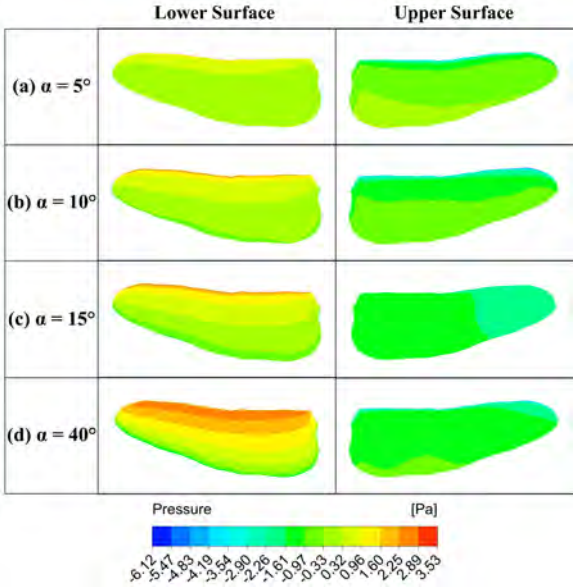

Figure 11 Reference planes (see online version for colours)

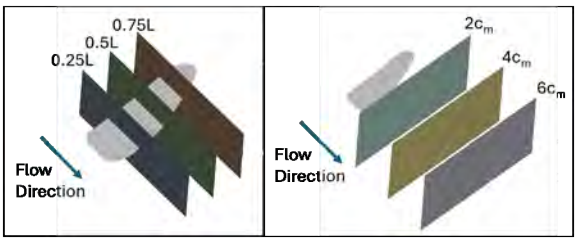

(a) (b)

Additional studies were carried out for Reynolds number 10,000 to compare the experimental findings of Kesel (2000). Figure 8 shows the comparison of previous studies by Chen and Skote (2016), model A (corrugated hind wing) and model B (profiled hind wing), and experimental studies by Kesel (2000) for flat plate and profiled wing with our wing model (model 1) for comparison with experimental

results for the profiled wing and flat plate. These results are relevant to insect wings, whose profiles are more similar to flat plates than airfoils. The present study considers a profiled hind wing of a dragonfly, as discussed in Section 2, and is similar to model B (Chen and Skote, 2016).

Figure 12 Streamlines for different values of α at Re 1,400 (see online version for colours)

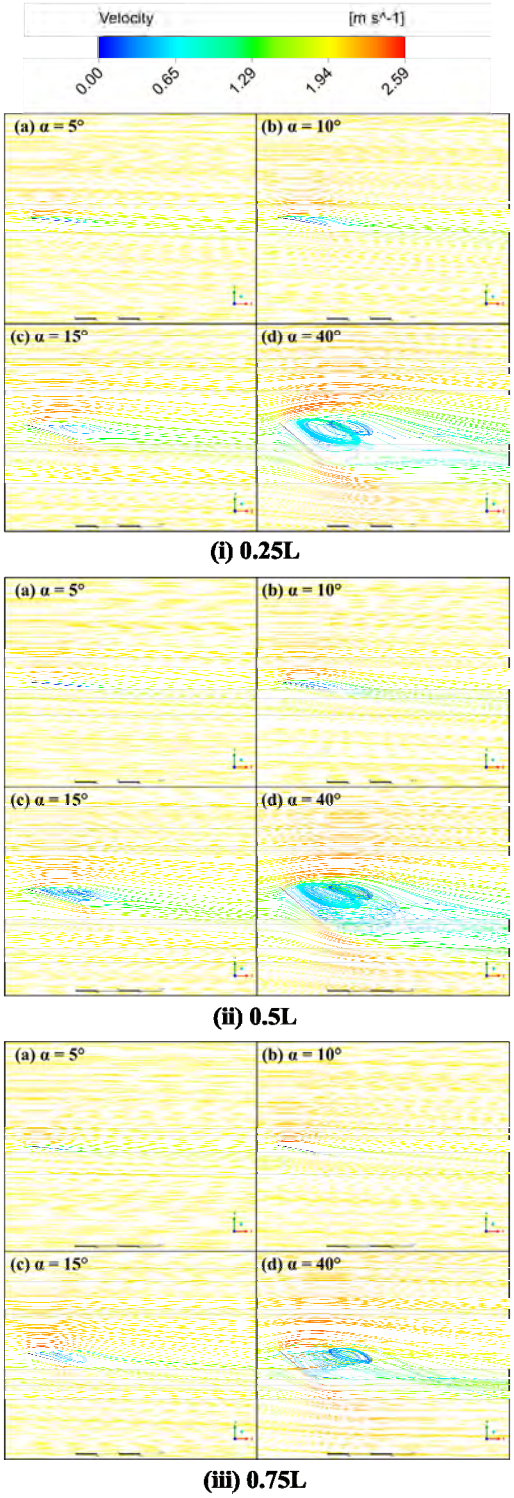

Figure 9 compares Reynolds numbers 550, 1,400, and 10,000 for our wing model. The flow separation or stall occurs beyond α = 10° for Reynolds numbers 550 and 1,400. Meanwhile, for Reynolds, the number of 10,000 stalls takes place at α = 5°. Hence, the insects fly at a lower Reynolds number for a broader range of α. From Figure 9, it is seen that there is an improvement in the glide ratio by nearly 30% as the Reynolds number is increased from 550 to 1,400. By setting the wings at a 10° angle of attack, the dragonfly can maximise its glide efficiency and maintain stable flight during wind gusts. Since the Reynolds numbers (1,400 and 550) lie in the same flow regime and have similar characteristics, we consider only 1,400 to present the following results.

Figure 13 Vorticity streamwise component showing the tip vortex Re 1,400 (see online version for colours)

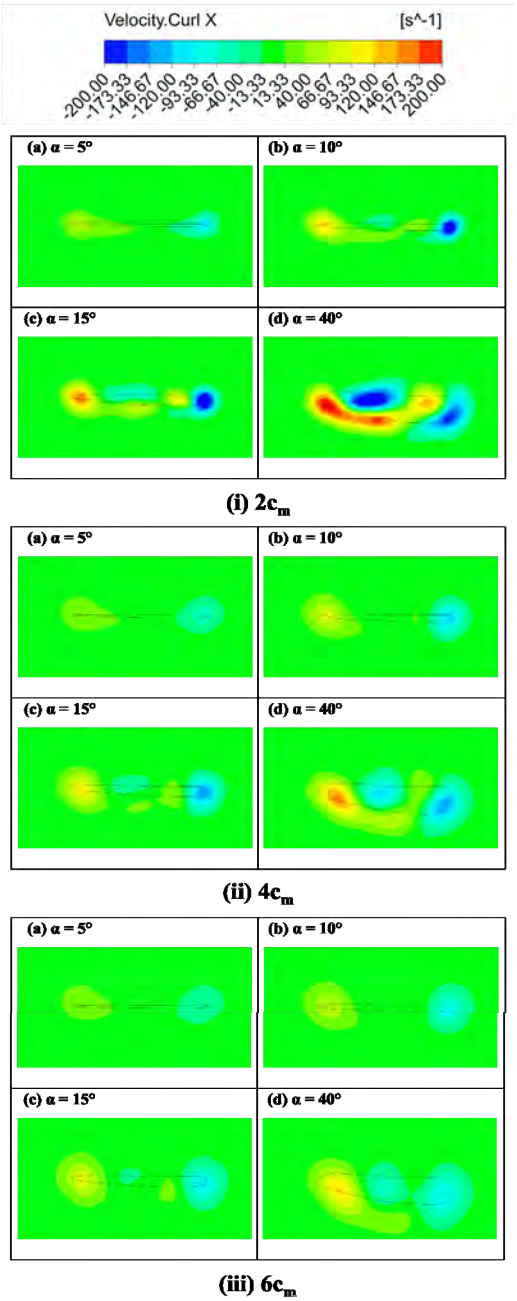

Figure 10 shows the pressure distribution along the wing surfaces, upper and lower. Suction pressure is developed on the upper surface. For lower values of α (5°, 10°), the pressure difference aids lift generation.

Figure 11(a) shows the reference planes along the chord at 0.25 L, 0.5 L, and 0.75 L, where L is the wing length from the wing root, And Figure 11(b) shows the reference planes along the streamwise direction at 2 cm, 4 cm, and 6 cm. From the streamlines shown in Figure 12(i) for different angles of attack at 0.25 L, it can be seen that the laminar flow separates as the angle of attack is increased from 5° to 40° degrees. This separation is also seen in Figure 12(ii) (0.5 L) and 12(iii) (0.75 L) as we move towards the tip. The vortices formed in the wake region of the separated flow are visible at a 40° angle of attack.

As the angle of attack (α) increases, tip vortices begin to form at the wingtips due to differences in pressure between the upper and lower surfaces. These tip vortices are visualised by the vorticity streamwise component (Velocity.Curl X), as shown in Figure 13. The vorticity is captured along the wake at reference planes discussed in Figure 11(b). As the vortices grow in strength with higher angles of attack, airflow patterns around the wing are altered. The intensified tip vortices induce a higher level of circulation around the wing, increasing induced drag. This induced drag, which is a significant component of total drag, adversely affects the glide performance.

This study suggests that during wind gusts, the dragonfly can maintain its flight by utilising a gliding strategy. This is an effective way for the dragonfly to remain airborne and navigate through turbulent air.

The findings of this study have the potential to be applied to the design and operation of insect-scale aerial vehicles. These small drones are often inspired by the flight capabilities of insects. By mimicking the dragonfly's gliding and wing orientation strategies, these aerial vehicles could conserve energy during wind gusts and maintain stable flight, even in challenging weather conditions.

5 Conclusions

The methodology to obtain the wing morphology using a digital camera, micrometer, and SEM has been explained in this study. The thickness reduces from the wing root to the wing tip and from the leading edge to the trailing edge, as seen in aircraft wings, thus improving aerodynamic performance. The gliding aerodynamics is studied for Reynolds numbers 1,400 and 550. The flow separation affects the angle of attack beyond 10°, and a fully separated flow is visible for a 40° angle of attack. The Reynolds numbers 550 and 1,400 showed the maximum glide ratio near α = 10°. Hence, considering the Reynolds number for actual dragonfly flight that is below 2,400, the wing orientation to sustain flight, the dragonfly, would have to orient the wing to have an angle of attack of 10°.

Acknowledgements

The authors extend their appreciation to the Deanship of Research and Graduate Studies at King Khalid University for collaboration and support.

The authors express their gratitude to the Center of Excellence in Avionics and Navigation, Department of Aeronautical and Automobile Engineering, Manipal Institute of Technology, Karnataka, India, for their support.

References

4 Ways to Preserve Insects – wikiHow (n.d) [online] https://www.wikihow.com/Preserve-Insects (accessed 17 September 2021).

Bin Abas, M.F. et al. (2016) 'Flapping wing micro-aerial-vehicle: kinematics, membranes, and flapping mechanisms of ornithopter and insect flight', *Chinese Journal of Aeronautics*, Vol. 29, No. 5, pp.1159–1177, DOI: 10.1016/J.CJA.2016.08.003.

Boughou, S. et al. (2023) 'Numerical investigation on the aerodynamics of high-lift and bird-like low Reynolds number airfoils', *Progress in Computational Fluid Dynamics*, Vol. 23, No. 3, pp.146–162, DOI: 10.1504/PCFD.2023.131027.

Chen, Y.H. and Skote, M. (2016) 'Gliding performance of 3-D corrugated dragonfly wing with spanwise variation', *Journal of Fluids and Structures*, Vol. 62, pp.1–13, DOI: 10.1016/J.JFLUIDSTRUCTS.2015.12.012.

Gaissert, N. et al. (2013) 'Inventing a micro aerial vehicle inspired by the mechanics of dragonfly flight', *Lecture Notes in Computer Science (including subseries Lecture Notes in Artificial Intelligence and Lecture Notes in Bioinformatics)*, 8069 LNAI, pp.90–100, DOI: 10.1007/978-3-662-43645-5_11.

Gibbs-Smith, C.H. (1974) 'Sir George Cayley, Father of Aerial Navigation (1773-1857)', *The Aeronautical Journal*, Vol. 78, No. 760, pp.125–133, DOI: 10.1017/S0001924000088746.

He, F. et al. (2023) 'Numerical comparison of laminar flow and turbulence models of hemodynamics based on pulmonary artery stenosis', *Progress in Computational Fluid Dynamics*, Vol. 23, No. 5, pp.317–325, DOI: 10.1504/PCFD.2023.134209.

Heinrich, B. (1993) 'Dragonflies now and then', in *The Hot-Blooded Insects: Strategies and Mechanisms of Thermoregulation*, pp.117–142, Springer Berlin Heidelberg, Berlin, Heidelberg, https://doi.org/10.1007/978-3-662-10340-1_4.

Jakab, P.L. (2012) 'Otto Lilienthal: 'The Greatest of the Precursors'', *AIAA Journal*, Vol. 35, No. 4, pp.601–607, https://doi.org/10.2514/2.154.

Jongerius, S.R. and Lentink, D. (2010) 'Structural analysis of a dragonfly wing', *Experimental Mechanics 2010*, Vol. 50, No. 9, pp.1323–1334, DOI: 10.1007/S11340-010-9411-X.

Kesel, A.B. (2000) 'Aerodynamic characteristics of dragonfly wing sections compared with technical aerofoils', *Journal of Experimental Biology*, Vol. 203, No. 20, pp.3125–3135, DOI: 10.1242/JEB.203.20.3125.

Khader, S.M.A. et al. (2018) 'Haemodynamics behaviour in normal and stenosed renal artery using computational fluid dynamics', *Journal of Advanced Research in Fluid Mechanics and Thermal Sciences*, Vol. 51, No. 1, pp.80–90.

Livya, E., Anitha, G. and Valli, P. (2015) 'Aerodynamic analysis of dimple effect on aircraft wing', *International Journal of Aerospace and Mechanical Engineering*, Vol. 9, No. 2, pp.350–353.

May, M.L. (1978) 'Thermal adaptations of dragonflies', *Odonatologica*, Vol. 7, No. 1, pp.27–47.

May, M.L. (1991) 'Thermal adaptations of dragonflies, revisited', *Advances in Odonatology*, Vol. 5, No. 1, pp.71–88.

Mizrahy-Rewald, O. et al. (2022) 'Empirical evidence for energy efficiency using intermittent gliding flight in northern bald ibises', *Frontiers in Ecology and Evolution*, Vol. 10, p.523, DOI: 10.3389/FEVO.2022.891079/BIBTEX.

Okamoto, M., Yasuda, K. and Azuma, A. (1996) 'Aerodynamic characteristics of the wings and body of a dragonfly', *Journal of Experimental Biology*, Vol. 199, No. 2, pp.281–294, DOI: 10.1242/JEB.199.2.281.

Peskin, C.S. (1977) 'Numerical analysis of blood flow in the heart', *Journal of Computational Physics*, Vol. 25, No. 3, pp.220–252, DOI: 10.1016/0021-9991(77)90100-0.

Rival, D., Schönweitz, D. and Tropea, C. (2011) 'Vortex interaction of tandem pitching and plunging plates: a two-dimensional model of hovering dragonfly-like flight', *Bioinspiration & Biomimetics*, Vol. 6, No. 1, p.016008, DOI: 10.1088/1748-3182/6/1/016008.

Sachs, G. (2017) 'Energy saving of aerial roosting Swifts by dynamic flap-gliding flight', *Journal of Ornithology*, Vol. 158, No. 4, pp.943–953, DOI: 10.1007/S10336-017-1447-6/FIGURES/8.

Sachs, G. (2022) 'Powered-gliding/climbing flight', *Journal of Theoretical Biology*, Vol. 547, p.111146, DOI: 10.1016/J.JTBI.2022.111146.

Sett, R., Verekar, P.P. and Zuber, M. (2023) 'Comparative study of dimple effect on three-dimensional cambered aircraft wing', *Journal of Advanced Research in Fluid Mechanics and Thermal Sciences*, Vol. 104, No. 2, pp.115–126, DOI: 10.37934/ARFMTS.104.2.115126.

Simmons, P. (1977) 'The neuronal control of dragonfly flight. I. Anatomy', *Journal of Experimental Biology*, Vol. 71, No. 1, pp.123–140, DOI: 10.1242/JEB.71.1.123.

Singh, S. et al. (2022) 'Classification of actuation mechanism designs with structural block diagrams for flapping-wing drones: a comprehensive review', *Progress in Aerospace Sciences*, Vol. 132, p.100833, DOI: 10.1016/J.PAEROSCI.2022.100833.

Singh, D.K., Parmar, D.L. and Sharma, A. (2023a) 'Flow separation control in a two-airfoil system by trailing edge modification and active flow control', *Progress in Computational Fluid Dynamics*, Vol. 23, No. 6, pp.352–363, DOI: 10.1504/PCFD.2023.134897.

Singh, S. et al. (2023b) 'Kinematic investigations of a novel flapping actuation design with mutually perpendicular 3 cylindrical joint approach for FW-drones', *Biomimetics*, Vol. 8, No. 2, p.160, DOI: 10.3390/BIOMIMETICS8020160.

Valerian Corda, J., Emmanuel, J. et al. (2023a) 'Airflow patterns and particle deposition in a pediatric nasal upper airway following a rapid maxillary expansion: computational fluid dynamics study', *Cogent Engineering*, Vol. 10, No. 1, DOI: 10.1080/23311916.2022.2158614.

Valerian Corda, J., Satish Shenoy, B. et al. (2023b) 'Micro-and nanoparticle transport and deposition in a realistic neonatal and infant nasal upper airway', *International Journal of Modelling and Simulation*, DOI: 10.1080/02286203.2022.2164155.

Wakeling, J. and Ellington, C. (1997) 'Dragonfly flight. I. Gliding flight and steady-state aerodynamic forces', *Journal of Experimental Biology*, Vol. 200, No. 3, pp.543–556, DOI: 10.1242/JEB.200.3.543.